



Model Predictive Control of an Irrigation Canal Using Dynamic Target Trajectory

Min Xu¹

Abstract: Model predictive control (MPC) has been extensively studied for controlling irrigation canals. Most of the studies use lumped models and fixed target for the controller. This setup works fine if the water delivery is on demand. However, in the case of on-supply delivery, balancing mismatches between demand and supply and spreading mismatches among all users are crucial. A fixed control target will not meet the request due to the mismatches. In this paper, a dynamic target trajectory approach is proposed to calculate changes of control targets that are used by MPC. The dynamic target trajectory calculates the percentage change of each setpoint based on the total volume mismatch spreading over the available capacity in each canal pool. The approach is applied to the Central Main Canal in Arizona. The results demonstrate that the dynamic trajectory can help the optimization find the optimum more quickly and facilitate tuning of the controller. Moreover, the mismatches can be better distributed over canal pools. **DOI: 10.1061/(ASCE)IR.1943-4774.0001084.** © 2016 American Society of Civil Engineers.

Author keywords: Dynamic target trajectory; Integrator-delay model; Irrigation canal; Model predictive control.

Introduction

As clean water is becoming a scarce resource, efficient water delivery is more and more important. Efficient delivery necessitates that the requested amount of water be delivered at the required moment. In irrigation systems, traditional manual operation and supervisory manual control are still employed based on the skills and experience of operators (Rogers and Goussard 1998). Supervisory manual control allows the water master to monitor system conditions and to manipulate control structures from a headquarter office. Some feedback-control algorithms, such as the proportional-integral (PI) controller, are also widely applied to manage water delivery based on current measurements (Burt et al. 1998; Schuurmans et al. 1997, 1999; Litrico et al. 2003). However, these control methods cannot meet the increasing standard of efficient water delivery and may cause water losses. Thus, more advance control technique is required to better operate irrigations canals.

In the last decades, model predictive control (MPC), which originated from industrial engineering in the 1970s, was introduced to controlling water systems. It has been successfully applied to control irrigation canals, rivers, and reservoirs (Brian and Clemmens 2006; Blanco et al. 2010; Tian et al. 2015; Schwanenberg et al. 2014). It is used not only for water quantity control but also for water quality regulation (Xu et al. 2010). The MPC uses a model to predict future system dynamics and solves a control problem with optimization, considering system constraints over a finite prediction horizon (Camacho and Alba 2013). The accuracy and complexity of the prediction model largely affect the control performance of MPC in terms of control accuracy and computation time.

In control of irrigation canals, integrator-delay (ID) model is commonly used in MPC to simplify optimization, such as (van Overloop et al. 2005; Clemmens and Schuurmans 2004). The ID model is linear and contains two parts: delay of water transport from upstream to downstream, and (reservoir) integrator, which represents mass balance (Schuurmans et al. 1995). Delay steps and reservoir characteristics (water surface area when water level is at setpoint) are precalculated based on a certain flow condition. This creates the main drawback of the ID model, which is that the model is not able to adapt large flow fluctuations that change the delay time and the water surface area.

In most controls of water systems, fixed setpoints are used as control targets. In irrigation canals, these targets guarantee enough water extraction through offtakes. However, when mismatches occur between supply and demand, the fixed target has to be violated. In this case, it is not necessary to keep setpoints fixed over time. In this paper, a dynamic target trajectory method is proposed to calculate dynamic setpoints over the simulation period. The calculation is based on total volume mismatches between supply and demand spreading over the available capacity in each canal pool. The available capacity is determined by the upper and lower operational or physical water level bounds. This method is expected to shorten the route of finding optimal solutions within optimization, which means reducing computation time. Due to the spreading of mismatches over pools, water levels can be better controlled. Moreover, the dynamic target trajectory method can also facilitate the tuning of weighing factors in MPC due to the consideration of the available capacity of each pool.

Model Predictive Control Using Dynamic Target Trajectory

Model Predictive Control

Model predictive control is a setup of a constrained optimization problem that uses a certain optimization algorithm to find optimal solutions of an objective function over a finite prediction horizon. The objective function is usually subject to both equality and

¹Researcher, Deltares, Boussinesqweg 1, 2629 HV, Delft, Netherlands. E-mail: min.xu@deltares.nl

Note. This manuscript was submitted on July 20, 2015; approved on April 18, 2016; published online on July 12, 2016. Discussion period open until December 12, 2016; separate discussions must be submitted for individual papers. This paper is part of the *Journal of Irrigation and Drainage Engineering*, © ASCE, ISSN 0733-9437.

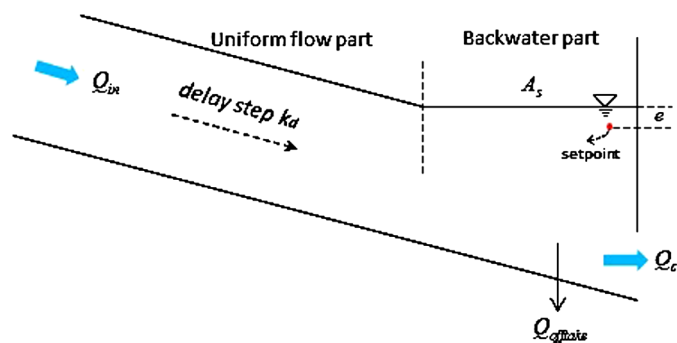


Fig. 1. ID model variables

inequality constraints. In closed-loop MPC, the first optimal solution over the prediction horizon is implemented in practice and the optimization is executed at each control step as time proceeds forward. An optimization problem setting can be formulated as follows:

$$J = \min_u (X'QX + U'RU)$$

$$\text{subject to } \begin{cases} x(k+1) = Ax(k) + B_u u(k) + B_d d(k) \\ u_{\min} \leq u(k) \leq u_{\max} \\ k = 1, \dots, n \end{cases} \quad (1)$$

where X = state vector $[x(1), x(2), \dots, x(n)]$; U = control input vector $[u(1), u(2), \dots, u(n)]$; Q = weighing matrix on states; R = weighing matrix on control inputs; A = state matrix; B_u = control input matrix; B_d = disturbance matrix; d = disturbance; u_{\min} and u_{\max} = upper and lower bounds of control inputs; n = number of prediction steps; and k = time step index.

In the control of irrigation canals, the control objective on states is usually the water level deviations from targets, and objective on control inputs is the change of control flow in order to minimize wear and tear of hydraulic structures. The objective function is usually quadratic in order to balance both positive and negative deviations (van Overloop 2006). Such an optimization problem can be solved through quadratic programming.

The equality constraints of Eq. (1) are called the state-space model, which can be represented by an integrator-delay model in canal control, assuming a constant control target

$$e(k+1) = e(k) + \frac{T_c}{A_s} \{Q_{in}(k-k_d) - [Q_c(k) + Q_{offtake}(k)]\} \quad (2)$$

where e = water level deviation from the target; k_d = number of delay steps; T_c = control time step; A_s = water surface area; Q_{in} = inflow; Q_c = control flow; and $Q_{offtake}$ = flow of farm offtake. Fig. 1 illustrates the ID model variables in Eq. (2).

Dynamic Target Trajectory

Considering the situation that water levels are far from setpoints at the end of the prediction time step but water demand is still higher than the supply (negative flow mismatches) in the system, optimization may find it difficult to achieve optimal solutions or even could not find feasible solutions without violating constraints. Because of the mismatches, it is not necessary to always keep a fixed setpoint over the prediction horizon and a dynamic target trajectory method is proposed to balance volume mismatches in a canal. The target trajectory will reduce the water level deviation from the setpoints at each time step based on the available capacity

of each pool, thus speeding up the process of finding optimal solutions.

In an on-supply delivery, all the flow mismatches are already known at the beginning, based on the timing and amount of water usage and delivery. At each time step, the setpoint of each pool can be calculated from the fixed setpoint and a percentage filling of the water level limit. The percentage filling is based on the upper and lower water level limits and the total potential storage that is the volume between the water level limits and the fixed setpoints for all pools. The calculation appears later in the paper.

The flow mismatch between supply and demand is converted into the volume mismatch over each control time step. The integral is calculated in the receding horizon

$$V_{\text{mis}}(k) = T_c \times \sum_{i=1}^k [Q_{in}(i) - \sum_{j=1}^m Q_{offtake,j}(i)] \quad (3)$$

where V_{mis} = volume mismatch between supply and demand; k = control step index; and m = number of offtakes.

This mismatch takes a certain percentage in the total potential storage. The percentage filling of limits can be formulated as

$$SP_{\text{perc},j}(k) = \frac{V_{\text{mis}}(k)}{\sum_{j=1}^p (A_j \times L_j)} \times L_j \quad (4)$$

where $SP_{\text{perc},j}$ = percentage filling of water level limit in the j th pool; A_j = water surface area of the j th pool when water is at fixed setpoint; L_j = operational water level limit of the j th pool, which is normally provided by canal administrator and time-invariant; and p = number of canal pools. Although the surface water area A_j at a fixed setpoint can vary under different flow conditions, it is assumed to be constant due to the fact that the ID model does not take varying water surface area and delay into account. This is the disadvantage of using the ID model in MPC.

When applying the percentage filling, the dynamic setpoint of each pool at time step k becomes

$$SP_j(k) = SP_{\text{fixed},j} + SP_{\text{perc},j}(k) \quad (5)$$

where SP = dynamic time-variant setpoint in the j th pool; and $SP_{\text{fixed},j}$ = fixed setpoint in the j th pool.

The setpoint change has no relationship with the fixed setpoint, but with its percentage filling

$$\begin{aligned} \Delta SP_j(k) &= SP_j(k) - SP_j(k-1) = SP_{\text{perc},j}(k) - SP_{\text{perc},j}(k-1) \\ &= \frac{V_{\text{mis}}(k)}{\sum_{k=1}^p (A_j \times L_j)} \times L_j - \frac{V_{\text{mis}}(k-1)}{\sum_{k=1}^p (A_j \times L_j)} \times L_j \end{aligned} \quad (6)$$

where ΔSP_j = setpoint change in the j th pool.

Application of Dynamic Target Trajectory in MPC

In the dynamic target trajectory method, water level deviation is calculated from the dynamic setpoint and it becomes

$$e(k) = h(k) - SP(k) \quad (7)$$

When Eq. (7) is substituted into the integrator-delay model Eq. (2) and the change of flow is considered as the control input instead of the flow itself, Eq. (2) becomes

$$e(k+1) = e(k) + \frac{T_c}{A_s} \{Q_{in}(k - k_d) - [Q_c(k-1) + \Delta Q_c(k) + Q_{offtake}(k)]\} - \Delta SP(k+1) \quad (8)$$

The setpoint change is considered an extra disturbance to the system and joins into the disturbance matrix. Thus, the state-space equation using dynamic setpoints over the prediction horizon can be rewritten as

$$X = Ax_0 + B_u U + B_d(D + D_e) \quad (9)$$

where D_e = extra disturbance vector containing the changes of setpoint.

The dynamic setpoint is updated for each time step before it comes into the MPC algorithm. In the optimization, changes of setpoint act as a corrector that softens constraints and facilitates problem solving. When Eq. (9) is substituted into the objective function Eq. (1), it becomes

$$J = \min_U [X' Q X + U' R U + (B_d D_e)' Q (2X + B_d D_e)] \quad (10)$$

For optimization, the minimum of the objective function can be found at the point where the gradient of the function is zero when applying quadratic programming (Fletcher 2013). The Hessian matrix H and the Lagrangian f in solving the optimization problem can be derived as follows (detailed deduction is described in the Appendix):

$$\begin{aligned} H &= 2(B_u' Q B_u - R K B_u + R + B_u' K' R K B_u - B_u' K' R) \\ f &= 2x_0(A' Q B_u + A' K' R K B_u - A' K' R) \\ &\quad + 2(D + D_e)'(B_d' Q B_u + B_d' K' R K B_u - B_d' K' R) \end{aligned} \quad (11)$$

Test Case

The central main canal (CMC) is one of the main human-made irrigation canals in the Eloy district of Arizona, operated by the Central Arizona Irrigation and Drainage District (CAIDD). It takes water from the Central Arizona Project (CAP), and water in the canal flows by gravity. The canal has a concrete bottom liner and the total length is over 28 km with a design capacity of 25.47 m³/s. The canal is divided into seven pools of different lengths by six inline gates. There are 20 offtakes spreading along the canal. Fig. 2 demonstrates a top view and longitudinal profile [generated from a Google maps (2016) and a SOBEK model (Delft Hydraulics 2004)] of the CMC. Many culverts are constructed in the canal because the canal passes through areas that feature, for example, railways, large washes (drainage), and roads. Table 1 shows the pool properties of the canal where the water surface areas and delay time are calculated based on 50% of the canal maximal flow. The upper and lower bounds are relative to the setpoints. The determination of these bounds is based on the operational water level limits, which are normally provided by canal administrators.

The CMC is remotely manually operated through a feedforward control with the help of a supervisory control and data acquisition (SCADA) system. Farmers in that district should order their water one day in advance, and the information including the amount of water and the time of taking the water is sent to the central office.

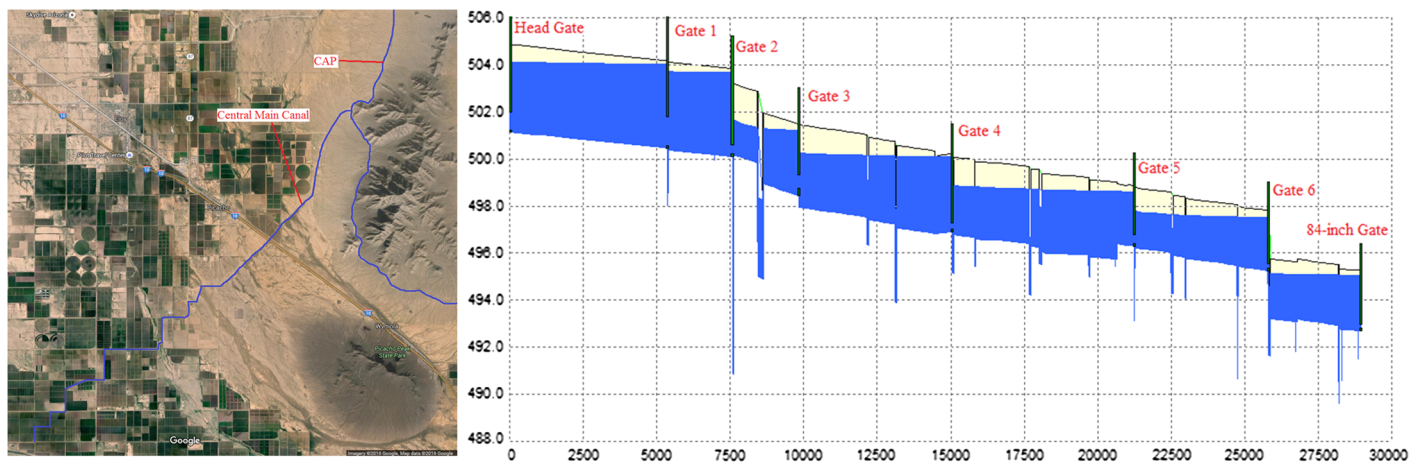


Fig. 2. Top view and longitudinal profile of CMC (Imagery ©2016 Google, Map data ©2016 Google)

Table 1. Pool Properties of CMC

Parameter	Pool 1	Pool 2	Pool 3	Pool 4	Pool 5	Pool 6	Pool 7
Length (m)	5,217.8	2,207.2	2,269.4	5,204.7	6,189.8	4,572.4	3,144.9
Water surface area (m ²)	67,016.3	30,218.4	18,750.1	57,775.6	57,036.1	31,707.8	22,739.0
Delay time (s)	180	15	180	375	645	510	270
Setpoint (m)	504.024	503.677	501.231	500.091	498.613	497.507	495.060
Upper bound (m)	0.213	0.213	0.152	0.244	0.152	0.213	0.305
Lower bound (m)	0.152	0.152	0.305	0.366	0.122	0.213	0.305

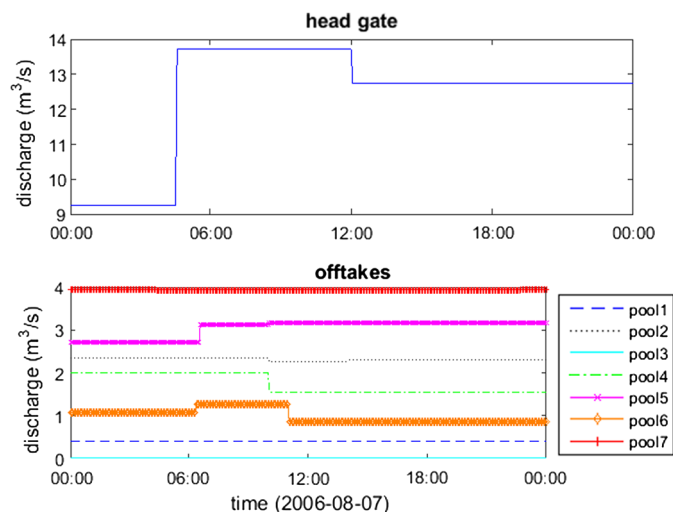


Fig. 3. Inflow at the canal head gate and flow demand of offtakes on August 7, 2006

Table 2. Flow Mismatches on August 7, 2006

Time (hrs.)	Mismatch average flow (m ³ /s)	Mismatch volume (m ³)
0000–0430	−3.23	−52,267
0430–1000	0.82	16,264
1000–1200	1.32	9,524
1200–1400	0.56	4,068
1400–1800	0.54	7,728
1800–2400	0.54	11,591
Total	−0.036	−3,092

The district then orders water from the CAP based on the total farmers' orders, to match their requirements.

In practice, the canal head gate can only be adjusted twice a day, normally once in the morning and again in the afternoon. In general, offtake adjustments are scheduled at 1000, 1400, and 1800 hrs. during the day. However, each offtake can schedule the specific moment of water extraction. Therefore, a mismatch in the time between water supply and demand is created. The goal of canal control is to satisfy all offtakes as much as possible by controlling water levels to certain targets and to spread the mismatch equally over each canal pool.

The test period is August 7, 2006, which has a normal flow condition. Fig. 3 shows the flows for the canal head gate and offtakes. Based this information, Table 2 presents the flow mismatches computation during the day for the entire canal. The flow adjustments of the canal head gate at 0430 and 1200 hrs. are taken into account in the mismatch calculation and some offtakes do not follow normal adjustment moments. The total mismatch is −3,092 m³, which means water demand is higher than supply.

The MPC test ran a closed-loop simulation and both fixed and dynamic setpoints were used for comparison. For the test using fixed setpoints, both scaled and unscaled weighing factors on water level deviation of each pool were tested to compare the convenience of turning with dynamic target trajectory method using unscaled weighing factors. Tables 3 and 4 show the weighing factors used for the three tests. Weighing factors on control inputs are kept the same for all cases, based on the maximal flow of gate.

Table 3. Scaled and Unscaled State Weighing Factors for Fixed and Dynamic Setpoints Tests

Pool index	Fixed setpoints	Fixed and dynamic setpoints
	Q (scaled)	Q (unscaled)
Pool 1	$1/(0.152)^2$	$1/(0.05)^2$
Pool 2	$1/(0.152)^2$	
Pool 3	$1/(0.305)^2$	
Pool 4	$1/(0.366)^2$	
Pool 5	$1/(0.122)^2$	
Pool 6	$1/(0.213)^2$	
Pool 7	$1/(0.305)^2$	

Table 4. Weighing Factors for Controlled Gates

Gate index	R	Q_m (m ³ /s)
Gate 1	$1/(0.01Q_{m,1})^2$	23.55
Gate 2	$1/(0.01Q_{m,2})^2$	19.81
Gate 3	$1/(0.01Q_{m,3})^2$	19.13
Gate 4	$1/(0.01Q_{m,4})^2$	13.70
Gate 5	$1/(0.01Q_{m,5})^2$	7.36
Gate 6	$1/(0.01Q_{m,6})^2$	5.55

Note: Q_m = maximal flow through inline gate.

Results

Closed-loop control results are demonstrated in this section on control accuracy and computation time, comparing between fixed and dynamic setpoint methods using both scaled and unscaled weighing factors. Fig. 4 shows the controlled water level of each pool for the three cases: fixed setpoint using scaled and unscaled weighing factors (FSP-scaled, FSP-unscaled) and dynamic setpoint using unscaled weighing factors (DSP-unscaled).

The water level has large violations (about 10 cm) in Pools 1 and 5 using FSP-unscaled (blue line). When weighing factors are scaled, the water level is better controlled but Pool 4 still has a lower bound violation of 20 cm (green line). The best control performance is using dynamic setpoints. Water level follows the dynamic setpoint trajectory very well and can be controlled within the bound of each pool (red line), except Pool 1 with a maximal violation of 3 cm for 15 min. This violation happens at the moment when a large inflow change (almost 50% increase) occurs at the canal head gate. The violation can be mitigated or eliminated by setting up tighter weighing factor in pool one.

The dynamic target trajectory indicates the relative capacity of each pool. Because water levels are following the trajectories very well, Fig. 4 shows a better distribution of supply and demand mismatches over the pools using dynamic target trajectory method. It is also noticed that this method does not need complex tuning of the weighing factors because the relative capacity of each pool has already been considered in the optimization. For the fixed setpoint method (both scaled and unscaled), the control performance may be improved by fine-tuning weighing factors on the water level deviations, such as increasing the weight on Pool 4. However, all weights are related to each other. Increasing the weight on Pool 4 decreases relative weights on other pools, then it decreases the performance of other pools accordingly. It is preferred to use unscaled weighing factors for the convenience of tuning. The dynamic target trajectory method meets the requirements of both control accuracy and tuning convenience.

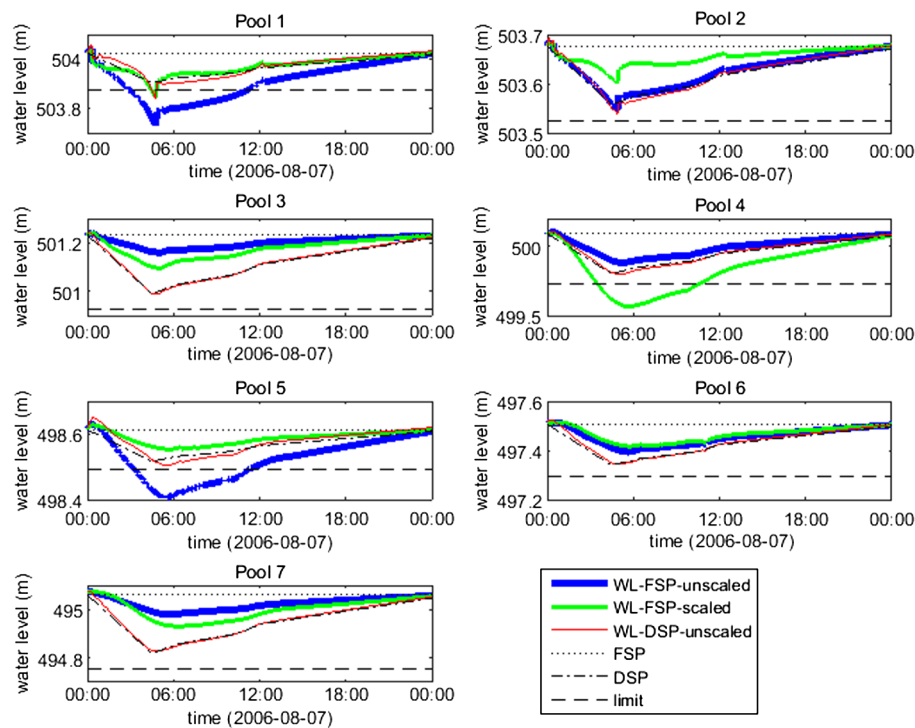


Fig. 4. Controlled water levels using both fixed and dynamic setpoints, as well as scaled and unscaled weighing factors

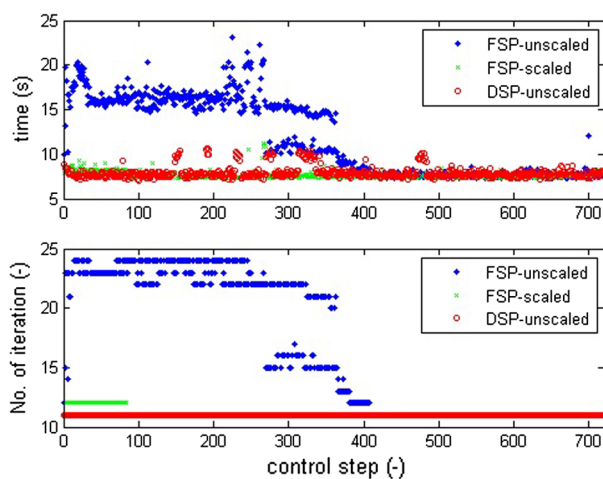


Fig. 5. Computation time and number of iterations of optimization algorithm in a closed-loop simulation

Another important criterion of control performance is computation time. Fig. 5 compares the computation time and the number of iterations of the optimization algorithm in a closed-loop simulation among the three methods. The DSP-unscaled and FSP-scaled methods take a similar amount of computation time, but almost half of one taken by the FSP-unscaled in the first half day. The time consumption of the two methods is relatively constant over the whole period. The large mismatches between supply and demand happen in the first half day, which includes the two flow changes at the canal head gate. Thus, including the relative capacity of each pool in the optimization can adapt the changes more quickly and stably.

Fig. 6 shows the controlled gate discharge using the dynamic target trajectory method. The canal head gate has two changes a

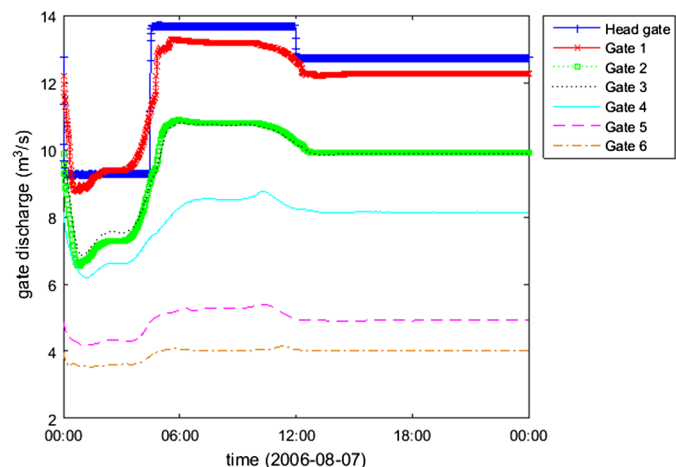


Fig. 6. Gate discharge with dynamic setpoints

day, and the first change is relatively large. Controlled discharge of each gate follows flow changes of the canal head gate very well and it is noticed that the gate discharges reduce from upstream to downstream due to the increase of farm offtakes. Fig. 6 also illustrates the advantage of prediction in MPC that prereleases water downstream due to the large inflow at 0430 hrs. Because the rate of change on gate discharges is used in the optimization, the gate flows adjust smoothly over the horizon.

Conclusions and Recommendations

The dynamic target trajectory method can be used to control an irrigation canal. It takes advantage of the setpoint change as an extra disturbance at each time step and performs as a correction of water

level deviations that softens system constraints in the optimization. This facilitates the optimization to find optimal solutions.

The dynamic target trajectory method uses percentage filling to calculate setpoint corrections and equally distributes the mismatches between supply and demand over the canal based on the available capacity of each pool. Because of the equal distribution of mismatches, a constant weighing factor can be applied to control states and fine tuning of specific canal pools is not necessary. This largely simplifies the tuning process in practice. Moreover, dynamic target trajectory method is more robust and stable of controlling all water levels within bounds and it is recommended in on-supply irrigation canal control.

The calculation of potential storage of each pool in Eq. (4) is based on water surface areas and operational limits. This

calculation is a rough estimation by using the backwater zone only, because the operational limits are normally specified at the downstream of each pool instead of along the pool. This rough estimation provides an increase or decrease trend of setpoints, which already performs better than commonly used fixed set points as shown in the results. However, for accurate calculation of the volume storage, both the backwater zone and delay part of the pool should be considered. This requires two model simulations with the same inflow condition. One simulation has downstream water levels controlled at setpoints, whereas the other has downstream water levels controlled at operational limits. Volume storage can be calculated based on the volume difference of the two simulations. This may lead to better control performance.

Appendix. Derivation of Hessian Matrix H and Lagrangian f

The objective function of the controlled system is

$$J = \min_U (X'QX + U'RU) \quad (12)$$

The state variables and the control actions are

$$\begin{aligned} X &= Ax_0 + B_u Z + B_d(D + D_e) \\ U &= -KX + Z = -K[Ax_0 + B_u Z + B_d(D + D_e)] + Z \end{aligned} \quad (13)$$

where K = feedback gain, which is not considered in this application (equals to 0). Substituting Eq. (13) into Eq. (12), it becomes

$$J = \min_U \left\{ [Ax_0 + B_u Z + B_d(D + D_e)]'Q[Ax_0 + B_u Z + B_d(D + D_e)] + \{-K[Ax_0 + B_u Z + B_d(D + D_e)] + Z\}'R\{-K[Ax_0 + B_u Z + B_d(D + D_e)] + Z\} \right\} \quad (14)$$

Based on the formation of $J(Z) = (1)/(2)Z'HZ + fZ + g$, only the terms consisting of Z or Z' should be considered in the equation. Therefore, rewriting Eq. (14) by neglecting the constant matrix g , for convenience, get the function of $J'(Z)$

$$\begin{aligned} J'(Z) &= x_0'A'QB_u Z + Z'B_u'Q[Ax_0 + B_d(D + D_e)] + Z'B_u'QB_u Z + (D + D_e)'B_d'QB_u Z + x_0'A'K'RKB_u Z - x_0'A'K'RZ \\ &\quad + Z'B_u'K'RK[Ax_0 + B_d(D + D_e)] + Z'B_u'K'RKB_u Z - Z'B_u'K'RZ + (D + D_e)'B_d'K'RKB_u Z \\ &\quad - (D + D_e)'B_d'K'RZ + Z'R[-KA_c x_0 + B_d(D + D_e)] - Z'RKB_u Z + Z'RZ \end{aligned} \quad (15)$$

Merging the terms containing Z and Z' will create the Hessian matrix, whereas extracting the terms only comprising of Z or Z' will generate the Lagrangian. The penalty matrices of Q and R are diagonal, which means that

$$\begin{aligned} Q &= Q' \rightarrow MQN = N'Q'M' = N'QM' \\ R &= R' \rightarrow MRN = N'R'M' = N'RM' \end{aligned}$$

when M and N have the same dimension. This gives many combinations of the previously mentioned terms. For example, the second term, $Z'B_u'QAx_0 = (Ax_0)'Q(Z'B_u')' = x_0'A'QB_u Z$, which is the same as the first term.

For optimization, the minimum of the objective function can be found at the point where the gradient of the function is zero when applying quadratic programming

$$\begin{aligned} J(U) &= \frac{1}{2}U'HU + fU + g \\ \frac{\partial J(U)}{\partial U} &= HU + f = 0 \\ U &= -\frac{f}{H} \end{aligned} \quad (16)$$

The Hessian matrix H and the Lagrangian f can be derived

$$\begin{aligned} H &= 2(B_u'QB_u - RKB_u + R + B_u'K'RKB_u - B_u'K'R) \\ f &= 2x_0(A'QB_u + A'K'RKB_u - A'K'R) \\ &\quad + 2(D + D_e)'(B_d'QB_u + B_d'K'RKB_u - B_d'K'R) \end{aligned} \quad (17)$$

Acknowledgments

This research was supervised by Dr. Peter-Jules van Overloop (1969–2015) from Delft University of Technology,

the Netherlands, and was denoted to memorialize his contributions in the field of canal automation.

References

- Blanco, T. B., Willems, P., Chiang, P. K., Haverbeke, N., Berlamont, J., and De Moor, B. (2010). "Flood regulation using nonlinear model predictive control." *Control Eng. Pract.*, 18(10), 1147–1157.
- Brian, W. T., and Clemmens, A. J. (2006). "Automatic downstream water-level feedback control of branching canal networks: Theory." *J. Irrig. Drain. Eng.*, 10.1061/(ASCE)0733-9437(2006)132:3(198), 198–207.
- Burt, C. M., Mills, R. S., and Khalsa, R. D. (1998). "Improved proportional-integral (PI) logic for canal automation." *J. Irrig. Drain. Eng.*, 10.1061/(ASCE)0733-9437(1998)124:1(53), 53–57.
- Camacho, E. F., and Alba, C. B. (2013). *Model predictive control*, Springer Science and Business Media, London.
- Clemmens, A. J., and Schuurmans, J. (2004). "Simple optimal downstream feedback canal controllers: Theory." *J. Irrig. Drain. Eng.*, 10.1061/(ASCE)0733-9437(2004)130:1(26), 26–34.
- Delft Hydraulics. (2004). *Sobek user guide and technical reference manual*, Delft, Netherlands.
- Fletcher, R. (2013). *Practical methods of optimization*, Wiley, Chichester, U.K.
- Google Maps. (2016). (maps.google.com) (May 19, 2016).
- Litrico, X., Fromion, V., Baume, J. P., and Rijo, M. (2003). "Modelling and PI control of an irrigation canal." *Proc., European Control Conf.*, IEEE, Piscataway, NJ, 850–855.
- Rogers, D. C., and Goussard, J. (1998). "Canal control algorithms currently in use." *J. Irrig. Drain. Eng.*, 10.1061/(ASCE)0733-9437(1998)124:1(11), 11–15.
- Schuurmans, J., Bosgra, O. H., and Brouwer, R. (1995). "Open-channel flow model approximation for controller design." *Appl. Math. Modell.*, 19(9), 525–530.
- Schuurmans, J., Hof, A., Dijkstra, S., Bosgra, O. H., and Brouwer, R. (1999). "Simple water level controller for irrigation and drainage canals." *J. Irrig. Drain. Eng.*, 10.1061/(ASCE)0733-9437(1999)125:4(189), 189–195.
- Schuurmans, J., Schuurmans, W., Berger, H., Meulenbergh, M., and Brouwer, R. (1997). "Control of water levels in the Meuse River." *J. Irrig. Drain. Eng.*, 10.1061/(ASCE)0733-9437(1997)123:3(180), 180–184.
- Schwanenberg, D., Xu, M., Ochterbeck, T., Allen, C., and Karimanzira, D. (2014). "Short-term management of hydropower assets of the Federal Columbia River power system." *J. Appl. Water Eng. Res.*, 2(1), 25–32.
- Tian, X., van Overloop, P. J., Negenborn, R. R., and van de Giesen, N. (2015). "Operational flood control of a low-lying delta system using large time step model predictive control." *Adv. Water Resour.*, 75, 1–13.
- van Overloop, P. J. (2006). *Model predictive control on open water systems*, IOS Press, Amsterdam, Netherlands.
- van Overloop, P. J., Schuurmans, J., Brouwer, R., and Burt, C. M. (2005). "Multiple-model optimization of proportional integral controllers on canals." *J. Irrig. Drain. Eng.*, 10.1061/(ASCE)0733-9437(2005)131:2(190), 190–196.
- Xu, M., van Overloop, P. J., van De Giesen, N., and Stelling, G. (2010). "Real-time control of combined surface water quantity and quality: Polder flushing." *Water Sci. Technol.*, 61(4), 869–878.